P 6.9

FREEZING DRIZZLE FORMATION OVER THE OREGON CASCADES DURING IMPROVE II

R.M. Rasmussen[1*], K. Ikeda[1], G. Thompson[1], and I. Geresdi[2]

[1]National Center for Atmospheric Research, Boulder, Colorado
[2]University of Pecs, Hungary

1. INTRODUCTION

A number of recent field programs have focused on the meteorological conditions leading to aircraft icing (WISP: Rasmussen et al. (1992), CFDE: Isaac et al. (1999), NASA Glenn, Miller et al. 1998). These programs have primarily focused on aircraft icing conditions over relatively flat terrain (Front Range of Colorado, New Foundland, and Cleveland) in association with cold fronts, warm fronts, and other features associated with mid-latitude cyclones (Bernstein et al. 1997). One of the key results coming out of these and other studies is the significantly higher frequency of freezing drizzle than previous thought (1 – 2% of all icing conditions versus 0.1% previously (Bernstein 2000, Rauber et al. 2000)). Freezing drizzle can be particularly hazardous to aircraft due to the impaction of the larger droplets beyond current deicing boots, leading to a significant reduction in aircraft performance that cannot be alleviated by the activation of ice protection devices such as pneumatic boots. These field programs have also shown that freezing drizzle is mostly formed via a collision-coalescence process rather then melting ice falling into below freezing air (Rasmussen et al. 1995, Cober et al. 1996, Rauber et al. 2000).

Recent climatologies of freezing drizzle by Bernstein (2000) and Stuart and Isaac (1999) have shown that freezing drizzle tends to maximize over continental regions close to large bodies of water, such as the Atlantic or Pacific oceans or the Great Lakes. For instance, freezing drizzle maxima are observed near Nova Scotia, Norway (Ben Bernstein, personal communication), Cleveland, the Pacific Northwest, and Alaska. This result is consistent with conventional thinking in cloud physics that the production of precipitation sized water drops through the collision-coalescence process is relatively rapid in maritime environments in which Cloud Condensation Nuclei (CCN) concentrations are low, leading to rapid broadening of the cloud droplet spectra to sizes at which the collision-coalescence process is rapid.

Corresponding author: Roy Rasmussen, National Center for Atmospheric Research, Boulder, CO, USA
Email: rasmus@ucar.edu

The results of icing studies in the above field programs have suggested that icing conditions (either supercooled liquid water or freezing drizzle), tends to be minimized when the radar reflectivity is greater than 5 dBZ. Since cloud droplets and drizzle have radar reflectivities less that 0 dBZ, the presence of 5 dBZ or greater typically indicates the presence of ice. Ice reduces liquid water and drizzle water content through depositional and accretional growth, thus limiting the build up of supercooled liquid water and drizzle (Geresdi et al. 2004). Since vertical motions in many of the icing clouds observed in previous icing programs are typically weak (< 10 cm/s) (Cober et al. 1996, Rasmussen et al. 1995, Murakami 1992), it does not take much ice to significantly deplete the water (freezing drizzle is typically not observed in regions in which ice crystal concentrations are greater than 0.1 L^{-1}, Rasmussen et al. 1995, Cober et al. 1996, Geresdi et al. 2004).Based on these results, icing diagnosis algorithms, such as the Current Icing Product (CIP; Bernstein et al. 2004) significantly reduce the probability of icing when the radar reflectivity is greater than 5 dBZ. However, a recent evaluation of the algorithm using Pilot Reports (PIREPS) of icing has shown a significant under-estimation of icing over the Pacific Northwest, especially over higher terrain regions. The recent IMPROVE II field program (Stoelinga et al 2003) provided an excellent opportunity to examine icing in this region, especially the presence of moderate or greater icing in regions of radar reflectivity greater than 5 dBZ. The IMPROVE II program involved two instrumented aircraft (University of Washington Convair and the NRL P-3), the S-Pol multi-parameter radar, a microwave radiometer, sounding sites, and other instruments (Stoelinga et al. 2003). Fig. 1 provides a schematic of the field program region and the location of the various facilities as well as the main aircraft tracks during the Nov. 28 storm. The goal of the IMPROVE II program was to improve bulk microphysical parameterizations over regions of mountainous terrain in order to better predict precipitation in these critical regions. In this paper we examine the post-frontal period of a winter storms during IMPROVE II in which freezing drizzle was observed. This post-frontal period had freezing drizzle in regions with high radar reflectivity (up to 20 dBZ) and moderate and greater icing and relatively warm cloud top temperatures (> -18 C).

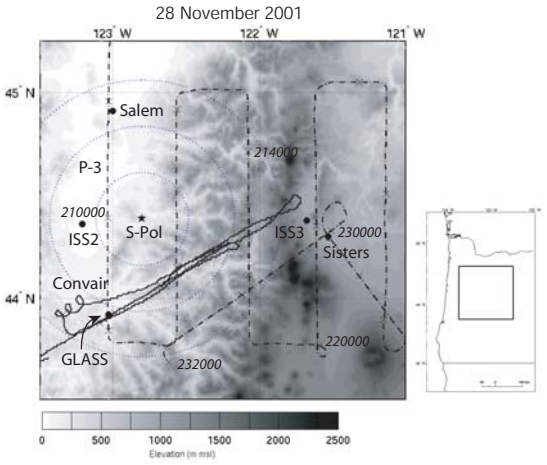

Figure 1: Topographic map of the study area. Convair (solid) and P-3's (dash-dot) flight tracks are overlaid. Crosses on the flight tracks are placed in a 10-minute inverval. Ground measurement sites are indicated by solid circles. Range rings are drawn every 25 km from the radar.

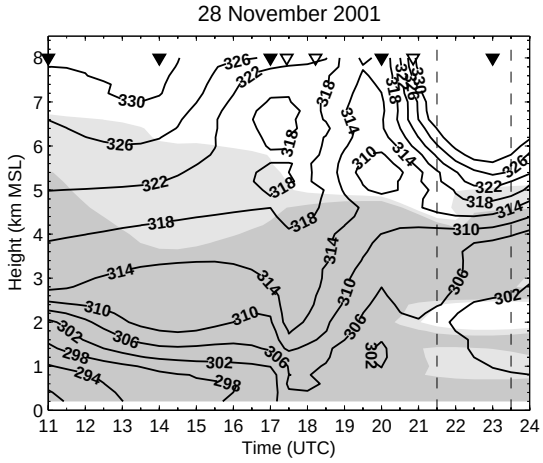

Figure 2: Time-height cross section of Θ_e (K) and relative humidity from the Salem and GLASS soundings on 28 November 2001. Dark (light) shaded is relative humidity above 80 % (between 70 and 80 %). Convair and P-3 were deployed between the times indicated by two vertical lines. Solid (open) triangles indicate the times of SLE (GLASS) soundings.

2. DESCRIPTION OF 28 NOVEMBER 2001 CASE

2.1 Synoptic and Mesoscale features

On 28 November a large synoptic low pressure system approached the northwest coast of the U.S. at 1200 UTC. With time the low pressure center took a northeastward track while the fronts swept across the coastal region from the southwest. Warm frontal clouds enveloped the northern Oregon Cascades between 0300 and 1200 UTC. The S-Pol radar images started to indicate light rain at this location prior to 0700 UTC. Infrared satellite images reveal the leading edge of cold frontal clouds moving southeastward over ISS2 (Fig. 1) at 1800 UTC. In the next one hour, the cold frontal clouds advanced just past the radar site (S-Pol). The cloud top temperature of the cold frontal clouds is between -10 and -20^{o}C, with a typical value of -15^{o}C. The warm frontal cloud, in contrast, exhibited cloud top temperatures between -40 and -50^{o}C.

The time-height cross-sections of equivalent potential temperature (Θ_e), relative humidity, wind direction, and wind speed (Fig. 2 from Salem) also indicate passage of warm frontal surface by 1300 UTC, suggested by the area of rapidly increasing Θ_e. Between 1400 and 1600 UTC, the lowest 1 km remains stable. Subsequently, the southwesterly winds intensify as the surface cold front approached and formed a barrier jet. The maximum speed of 45 m s^{-1} at 2 km MSL was recorded between 1700 and 1800 UTC at which time colder air associated with the front advanced. Behind the front (represented by the sloped surface of large Θ_e gradient), the lower atmosphere was nearly neutral. The top of the moist layer, which approximately indicates the cloud top height, at 1800 UTC was 5.3 km MSL and slowly descended to below 4 km. The 2300 UTC sounding showed a sub-saturated layer between 1.9 and 2.5 m MSL.

2.2. Aircraft Data

The Convair flew from 2134 to 2255 UTC on a northeast-southwest flight track, oriented nearly parallel to the mean wind flow during post-frontal conditions (Fig. 1). Level flight track altitudes were at 5.4 km (cloud top), 5.1 km, and 4.6 km. It performed two sets of vertical flight stacks, each consisting of two level flight legs.

The P-3 flew parallel to and 25 km south of Convair at an altitude of 4.2 km between 2300 and 2318 UTC. This flight track was over a region where the solid orographic cloud still prevailed. P-3 also performed a "lawnmower" flight pattern (Fig. 1) between 2030 and 2300 UTC intersecting the Convair's northeast-southwest flight track at four locations at heights 2, 2.6, 3.5, and 5 km (Fig. 3).

3. RESULTS

During the vertical aircraft stacks, the S-pol radar performed RHI scans over the eastern portion of the stack every 1 degree in azimuth between 81 and 141 degrees azimuth, repeating every 10 minutes. The advantage of this type of scan procedure is the high vertical resolution that can be achieved. In figure 3 we have re-constructed vertical cross sections of reflectivity along the

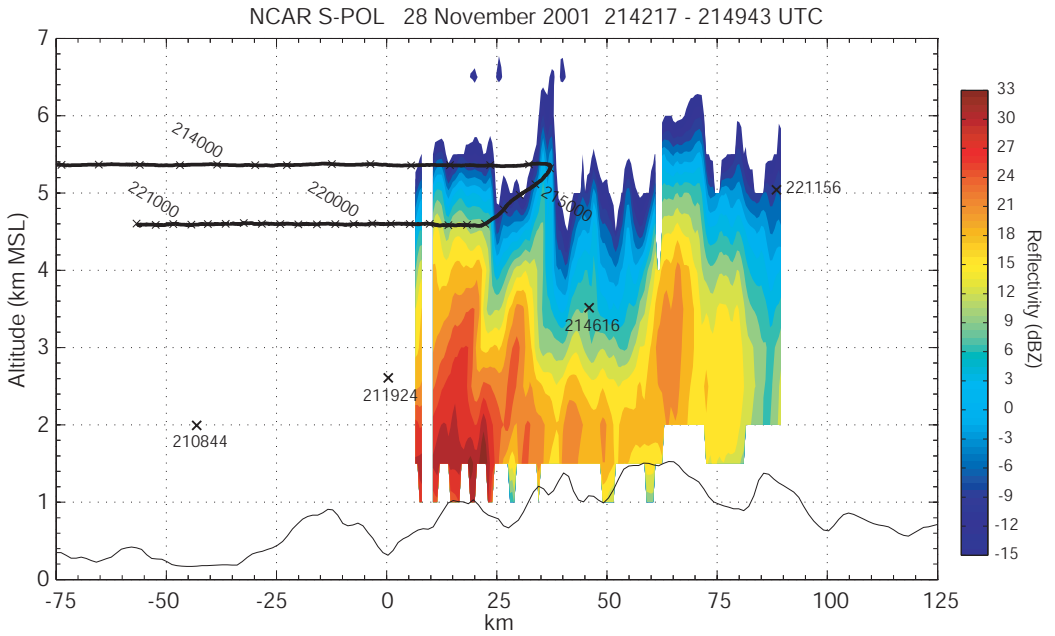

Figure 3: Reconstructed reflectivity RHI along Convair's Southwest-Northeast flight track between 213600 and 221200 UTC. The Convair flight track is indicated by a bold solid line. The crosses are placed every one minute. Four crosses at 2, 2.6, 3.5 and 5 km are locations that the P-3's north-south flight tracks intersected this vertical cross-section. Thin solid line is the topographic profile.

Convair aircraft stack every 10 minutes using these data. Over 61 scans were used to produce this RHI, thus the features are resolved with 2 km resolution. The first impression from these figures is the highly non-uniform nature of the radar echo along this vertical cross section. For example, there is a strong vertically coherent reflectivity maximum near 10 km horizontal distance, a second maximum near near 40, and a third near 75 km. Thus, there seems to be reflectivity maxima every 35 km or so. Examination of the cross sections every 10 minutes reveals that these maxima are moving with the mean winds in the layer at approximately 30 – 40 m/s (the lower level winds below 2.5 km height are , 30 m/s. The aircraft observer on the Convair aircraft noted that a convective cloud turrent was penetrated along the upper aircraft leg at 2146 UTC consisting of significant amounts of liquid water and ice corresponding to the first cloud penetration indicated in figure 3. Thus, the reflectivity maxima are most likely associated with embedded convection that is moving with the mean flow and generated by local ridges based on the fact that: 1) the lowest portion of the upstream sounding was convectively unstable, 2) the feature moved with the mean flow, and 3) the lifetime of each feature was on the order of 30 – 60 minutes or so.

Freezing drizzle is observed to occur just outside these reflectivity maxima. For instance, freezing drizzle is observed to occur during the cloud top penetrations shown in figure 3, and also at the two lower P-3 intersection points (211924 UTC and 214616 UTC). Each of these locations indicate the presence of freezing drizzle as indicated by spherical images between 100 and 300 microns diameter. In addition, the regions with radar reflectivity greater than 5 dBZ typically have snowflake aggregates present at sizes larger than 300 micons. Also note that drizzle is observed from – 3 to -18 C (other data not shown in this paper indicate the same result).

Since the air mass is maritime with a very low concentration of cloud droplets (< 30 cm^{-3} from the FSSP and the CCN counter), the cloud water value required to exceed before the onset of autoconversion is close to the observed value of 0.20 g/kg (Rasmussen et al. 2002). Drizzle formation typically occurs within 20 minutes for cumulus clouds with low concentrations of droplets (< 50 cm^{-3}), for example the shallow cumulus clouds upstream of Hawaii. Thus, the presence of drizzle in association with the embedded convection is entirely reasonable, especially when the ice crystal concentration is low and/or the updraft is over 0.5 m/s.

4. CONCLUSIONS

Microphysical conditions within a post-frontal cloud system during IMPROVE II are described based on aircraft, radar, and sounding data. The analysis showed that embedded convection was the

main mechanism producing significant vertical motion, cloud water, ice and drizzle. The embedded convection is most likely initiated by the deep vertical motion associated with flow over local ridges. Model simulations have verified this suggestion. Vertical motions were estimated to be between 0.5 to 1.5 m/s in the regions of cloud water maxima, significantly higher than 0.1 m/s values observed in the flat terrain storms. Thus, the higher condensate supply rate was able to maintain cloud water contents sufficiently high and for long enough periods to form drizzle in this maritime environment (typically cells lasted at least 30 minutes, drizzle onset was estimated to be 15-20 minutes). . A maritime environment allows drizzle to form for lower liquid water contents than for continental conditions (Rasmussen et al. 2002), allowing drizzle to form for the typically low water contents (< 0.2 gm^{-3}) observed in these storms.

Freezing drizzle was observed near cloud top in regions of low concentrations of ice crystals (< -5 dBZ), but also near the top of the main ridge where strong vertical motions were present and large snow aggregates. The reflectivity values in this case are on the order of 12 – 16 dBZ, significantly higher than typically observed with freezing drizzle. In this case, drizzle is able to survive the presence of ice crystal depletion due to the relatively strong vertical motions associated with the updrafts generated by the steep terrain. Thus, freezing drizzle and super-cooled liquid water can occur over complex terrain when the CCN concentration is low and the updrafts relatively high.

5. ACKNOWLEDGEMENTS

This research is in response to requirements and funding of the Federal Aviation Administration (FAA). The views expressed are those of the authors and do not necessarily represent the official policy of the FAA.

6. REFERENCES

Bernstein, B., T.A. Omeron, F. McDonough, and M.K. Politovich, 1997: The Relationship between Aircraft Icing and Synoptic-Scale Weather Conditions. *Wea. Forecasting*, **12**, 742 – 762.

Bernstein, B., T.A. Omeron, M.K. Politovich, and F. McDonough, 1998: Surface weather features associated with freezing precipitation and severe in -flight icing. *Atmos. Res.*, **46**, 57 – 73.

Bernstein, B. ,Frank McDonough, Marcia K. Politovich, Barbara G. Brown, Thomas P. Ratvasky, Dean R. Miller, Cory A. Wolff and Gary Cunning, 2004: Current Icing Potential (CIP): Algorithm Description and Comparison with Aircraft Observations. *J. Appl. Met*. (submitted).

Bernstein, B. C., 2000: Regional and local influences on freezing drizzle, freezing rain and ice pellet events, *Wea. Forecasting,* **15**, 485 – 508.

Cober, S. G., Strapp, and Isaac, G. A., 1996: An example of supercooled drizzle drops formed through a collision – coalescence process. *J. Appl. Met*., **35**, 2250-2260

Geresdi, I, R.M. Rasmussen, Woitek Grabowski, and Ben Bernstein, 2004: Sensitivity of Freezing Drizzle Formation in Stably Stratified Clouds to Ice Processes. *Meteorology and Atmospheric Physics*). (In Press)

Isaac, G.A., S.G. Cober, A.V. Korolev, J.W. Strapp, and A. Tremblay, 1999: Canadian Freezing Drizzle Experiment. 37th AIAA Aerospace Science Meeting and Exhibit, American Institute of Aeronautics and Astronautics, Paper AIAA-99-0492, 10 pp.

Miller, D., T. Ratvasky, B. Bernstein, F. McDonough, and J.W. Strapp, 1998:NASA/FAA/NCAR supercooled large droplet icing flight research: Summary of 96-97 flight operations. *36th Aerospace Science Meeting and Exhibit,* Reno, NV, American Institute of Aeronautics and Astronautics Paper AIAA 98-0557, 20 pp.

Murakami, M. Y. Yamada, T. Matsuo, H. Mizuno, and K. Morikawa, 1992: Microphysical structures of warm-frontal clouds. The 20 June 1987 case study. *J. Meteor. Soc. Japan*, **70**, 877 – 895.

Pruppacher, H. R. and Klett, J. D., 1997: Microphysics of clouds and precipitation. Kluwer Academic Publishers, 945

Rasmussen, R. M., Bernstein, B., Murakami, M., Stossmeister, G. and Stankov, B., 1995: The 1990 Valentine's Day Arctic Outbreak. Part I: Mesoscale and microscale structure and evolution of a Colorado Front Range shallow upslope cloud. *J. Appl. Met*., **34**, 1481-1511

Rasmussen, R, M., Geresdi, I., Thompson, G., Manning, K., and Karplus, E., 2002: Freezing drizzle formation in stably stratified layer clouds: The role of radiative cooling of cloud droplets and cloud condensation and ice initiation. *J. Atmos. Sci*., **59**, 837 – 860.

Rasmussen, R.M., M. Politovich, J. Marwitz, W. Sand, J. McGinley, J. Smart, R. Pielke, S. Rutledge, D. Wesley, G. Stossmeister, B. Bernstein, K. Elmore, N. Powell, E. Westwater, B. Stankov, and D. Burrows. 1992: Winter Icing and Storms Project (WISP). *Bull. Am. Meteorol. Soc*., **73**, 951 – 974.

Rauber, R.M., 1992: Microphysical structure and evolution of a central Sierra Nevada orographic cloud system. *J. Appl. Met*., **31**, 3 – 24.

Rauber, R.M., L.S. Olthoff, M.K. Ramamurthy, and K.E. Kunkel, 2000: The relative importance of warm rain and melting processes in freezing precipitation events. *J. Appl. Meteor*., **39**, 1185 – 1195.

Stoelinga, M.T., P.V. Hobbs, C.F. Mass, J.D. Locatelli, B.A. Colle, R.A. Houze, Jr., A.L. Rangno, N. A. Bond, B.F. Smull, R. M. Rasmussen, G. Thompson, B.R. Colman, 2003: Improvement of Microphysical Parameterization through Observational Verification Experiment. *Bull. Amer. Meteor. Soc.,* **84**, 1807 – 1826.

Stuart, R.A. and G.A. Isaac, 1999: Freezing Precipitation in Canada. Atmosphere-Ocean, 37, 87 – 102.

Vivekanandan, J., D. S. Zrnić, S. M. Ellis, R. Oye, A.V. Ryzhkov, and J. Straka, 1999: Cloud microphysics retrieval using S-band dual-polarization radar measurements. *Bull. Amer. Meteor. Soc.*, 80, 381-388.